

NUREG/CR-6191  
UILU-ENG-94-2002  
CARDIVNSWC-TR-61CR-94/01

---

---

# Size and Deformation Limits to Maintain Constraint in $K_{Ic}$ and $J_c$ Testing of Bend Specimens

DTIC QUALITY INSPECTED 4

---

---

Prepared by  
K. C. Koppenhoefer, R. H. Dodds, Jr.

University of Illinois

Naval Surface Warfare Center

Prepared for  
U.S. Nuclear Regulatory Commission

DISTRIBUTION STATEMENT A

Approved for public release  
Distribution Unlimited

95 SEP 13 P7:04

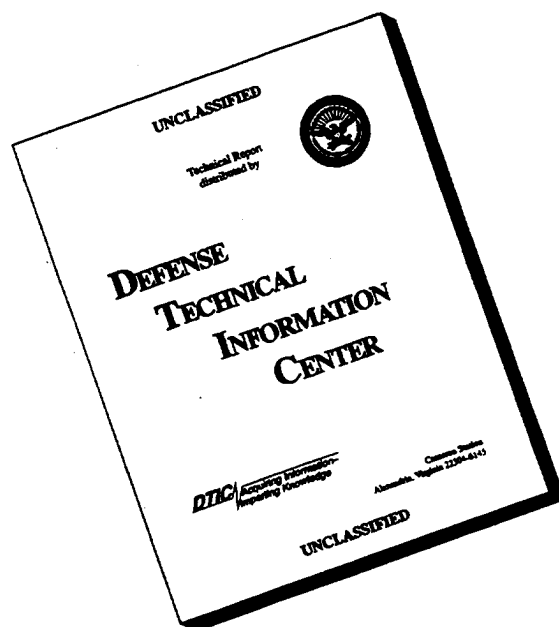
RECEIVED

9511270461 951031  
PDR NUREG  
CR-6191 R PDR

19960820 056

DF03  
0/1

# DISCLAIMER NOTICE



**THIS DOCUMENT IS BEST QUALITY AVAILABLE. THE COPY FURNISHED TO DTIC CONTAINED A SIGNIFICANT NUMBER OF PAGES WHICH DO NOT REPRODUCE LEGIBLY.**

## AVAILABILITY NOTICE

### Availability of Reference Materials Cited in NRC Publications

Most documents cited in NRC publications will be available from one of the following sources:

1. The NRC Public Document Room, 2120 L Street, NW., Lower Level, Washington, DC 20555-0001
2. The Superintendent of Documents, U.S. Government Printing Office, P. O. Box 37082, Washington, DC 20402-9328
3. The National Technical Information Service, Springfield, VA 22161-0002

Although the listing that follows represents the majority of documents cited in NRC publications, it is not intended to be exhaustive.

Referenced documents available for inspection and copying for a fee from the NRC Public Document Room include NRC correspondence and internal NRC memoranda; NRC bulletins, circulars, information notices, inspection and investigation notices; licensee event reports; vendor reports and correspondence; Commission papers; and applicant and licensee documents and correspondence.

The following documents in the NUREG series are available for purchase from the Government Printing Office: formal NRC staff and contractor reports, NRC-sponsored conference proceedings, international agreement reports, grantee reports, and NRC booklets and brochures. Also available are regulatory guides, NRC regulations in the *Code of Federal Regulations*, and *Nuclear Regulatory Commission Issuances*.

Documents available from the National Technical Information Service include NUREG-series reports and technical reports prepared by other Federal agencies and reports prepared by the Atomic Energy Commission, forerunner agency to the Nuclear Regulatory Commission.

Documents available from public and special technical libraries include all open literature items, such as books, journal articles, and transactions. *Federal Register* notices, Federal and State legislation, and congressional reports can usually be obtained from these libraries.

Documents such as theses, dissertations, foreign reports and translations, and non-NRC conference proceedings are available for purchase from the organization sponsoring the publication cited.

Single copies of NRC draft reports are available free, to the extent of supply, upon written request to the Office of Administration, Distribution and Mail Services Section, U.S. Nuclear Regulatory Commission, Washington, DC 20555-0001.

Copies of industry codes and standards used in a substantive manner in the NRC regulatory process are maintained at the NRC Library, Two White Flint North, 11545 Rockville Pike, Rockville, MD 20852-2738, for use by the public. Codes and standards are usually copyrighted and may be purchased from the originating organization or, if they are American National Standards, from the American National Standards Institute, 1430 Broadway, New York, NY 10018-3308.

## DISCLAIMER NOTICE

This report was prepared as an account of work sponsored by an agency of the United States Government. Neither the United States Government nor any agency thereof, nor any of their employees, makes any warranty, expressed or implied, or assumes any legal liability or responsibility for any third party's use, or the results of such use, of any information, apparatus, product, or process disclosed in this report, or represents that its use by such third party would not infringe privately owned rights.

---

---

# Size and Deformation Limits to Maintain Constraint in $K_{Ic}$ and $J_c$ Testing of Bend Specimens

---

---

Manuscript Completed: February 1994  
Date Published: October 1995

Prepared by  
K. C. Koppenhoefer, R. H. Dodds, Jr.

University of Illinois  
Department of Civil Engineering, MC-250  
205 North Mathews Avenue  
Urbana, IL 61801-2352

Under Contract to:  
Naval Surface Warfare Center  
Annapolis Detachment, Carderock Division  
Code 6140  
Annapolis, MD 21402-5067

S. Malik, NRC Project Manager

Prepared for  
Division of Engineering Technology  
Office of Nuclear Regulatory Research  
U.S. Nuclear Regulatory Commission  
Washington, DC 20555-0001  
NRC Job Code J6036

## ABSTRACT

The ASTM Standard Test Method for *Plane-Strain Fracture Toughness of Metallic Materials* (E399-90) restricts test specimen dimensions to insure the measurement of highly constrained fracture toughness values ( $K_{Ic}$ ). These requirements insure small-scale yielding (SSY) conditions at fracture, and thereby the validity of linear elastic fracture mechanics.

Recently, Dodds and Anderson have proposed a less restrictive size requirement for cleavage fracture toughness measured in terms of the  $J$ -integral ( $J_c$ ), as given by  $a, b, B \geq 200 J_c / \sigma_0$ . The size requirement proposed by Dodds and Anderson increases the applicability of fracture toughness experiments by expanding the range of conditions over which fracture toughness data meeting SSY conditions can be reliably measured. This investigation compares the proposed size requirement with that of ASTM Standard Test Method E399 and, by comparison with published experimental data for various alloys, provides validation of the new requirements.

# Contents

Section No.	Page
Abstract .....	iii
List of Figures .....	vi
List of Tables .....	vii
Acknowledgements .....	viii
1. NOMENCLATURE .....	1
2. INTRODUCTION .....	1
3. THEORETICAL BACKGROUND .....	2
3.1 Dodds-Anderson micromechanics model .....	2
3.2 $J$ - $Q$ theory .....	4
3.3 Statistical thickness effects .....	5
4. EVALUATION OF SIZE REQUIREMENTS .....	7
4.1 Materials and basis of comparison .....	7
4.2 Experimental data .....	8
5. SUMMARY AND DISCUSSION .....	10
6. REFERENCES .....	15

# LIST OF FIGURES

Figure No.		Page
1	Areas within principal stress contours for an $a/W = 0.15$ , $n=10$ SE(B). Values are normalized by area within contour for SSY at same $J$ -value .....	3
2	Variation of finite body-to-SSY $J$ with applied load for various strain hardening exponents in an $a/W = 0.5$ SE(B) specimen .....	4
3	Variation of $Q$ with applied load for an $a/W = 0.5$ SE(B) .....	6
4	Variation of fracture toughness with specimen thickness for A36 steel at $-76^{\circ}\text{C}$ .....	9
5	Variation of fracture toughness with crack depth for A36 steel at $-76^{\circ}\text{C}$ .....	10
6	Variation of fracture toughness with specimen thickness for A533-B at $-75^{\circ}\text{C}$ .....	11
7	Variation of fracture toughness with thickness for 18 Ni maraging steel .....	11
8	Variation of fracture toughness with specimen thickness for 4340 steel $a_0 = 28$ mm, $W = 56$ mm .....	12
9	Variation of fracture toughness with specimen thickness for 4340 steel $a_0 = 12.7$ mm, $W = 25.4$ mm .....	12
10	Variation of fracture toughness with specimen thickness for 4340 steel, $a_0 = 6.9$ mm, $W = 14$ mm .....	13
11	Variation of fracture toughness with thickness for Ti 6Al-6V-2Sn .....	14

# LIST OF TABLES

Table No.	Page
1 References for Experimental Data .....	7
2 Material properties and size ratios for experimental data .....	8



## **ACKNOWLEDGEMENTS**

This investigation was supported by grants principally from the Nuclear Regulatory Commission with additional support from Code 614, Annapolis Detachment, Carderock Division of the Naval Surface Warfare Center.

The authors wish to acknowledge the many useful discussions with Dr. Kim Wallin of the Technical Research Center of Finland.

## 1. NOMENCLATURE

$a$	crack length, mm
$b$	length of uncracked ligament, mm
$B$	specimen thickness, mm
$B_0$	normalizing thickness, mm
$\sigma_{ys}$	yield strength, MPa
$\sigma_{uts}$	ultimate tensile strength, MPa
$\sigma_0$	flow strength (average of yield and ultimate strength), MPa
$E$	Young's modulus, MPa
$\nu$	Poisson's ratio
$r, \theta$	polar coordinates from crack tip
$T$	stress parallel to the crack, MPa
$\delta_{ij}$	Kronecker delta
$Q$	higher order term of an asymptotic series; a stress triaxiality parameter
$K_{corr}$	fracture toughness corrected for statistical thickness effects, $\text{MPa}\sqrt{\text{m}}$
$K_{min}$	threshold fracture toughness, $\text{MPa}\sqrt{\text{m}}$
$K_I$	experimental fracture toughness, $\text{MPa}\sqrt{\text{m}}$
$K_q$	provisional fracture toughness value, $\text{MPa}\sqrt{\text{m}}$
$K_{Ic}$	specimen size independent fracture toughness value, $\text{MPa}\sqrt{\text{m}}$
$J_c$	experimental fracture toughness, $\text{kJ/m}^2$
$J_{corr}$	fracture toughness corrected for statistical thickness effects, $\text{kJ/m}^2$

## 2. INTRODUCTION

The ASTM Standard Test Method for *Plane-Strain Fracture Toughness of Metallic Materials* (E399-90) [1] restricts specimen dimensions relative to the deformation at fracture to insure that measured fracture toughness values ( $K_{Ic}$ ) correspond to highly constrained crack-tip conditions. These requirements are as follows:

$$a, b, B \geq 2.5 \left( \frac{K_q}{\sigma_{ys}} \right)^2 \quad (1)$$

Satisfaction of Eq (1) insures small-scale yielding (SSY) conditions at fracture, and thereby validates the assumptions of linear elastic fracture mechanics. The approximate diameter of the plastic zone under conditions given by Eq (1),

$$d_p \geq \frac{1}{3\pi} \left( \frac{K_q}{\sigma_{ys}} \right)^2 \quad (2)$$

is nearly 25 times smaller than relevant specimen dimensions. This degree of plastic zone confinement, set by the 2.5 multiplier in Eq (1), is based on experimental  $K_{Ic}$

data for many different metals. These data confirm that specimens satisfying Eq (1) produce equivalent (within scatter) fracture toughness values. However, different materials do not all indicate the need for a multiplier as severe as 2.5. Rolfe and Novak [2] and Facuher and Tyson [3] found that the 2.5 value could be reduced to as low as 1.0 for certain steel alloys (e.g. 18 Ni Maraging steel, micro-alloyed Lloyds LT-60). In contrast, Jones and Brown [4] presented data on titanium alloy 6Al-6Vn-2Sn in the aged condition demonstrating the need for the 2.5 value. To maintain a test standard independent of specific material, ASTM Committee E08 retains the more restrictive 2.5 value.

Recently, Dodds and Anderson [5] (hereafter referred to as DA) have proposed an alternative size requirement for cleavage fracture toughness measured in terms of the  $J$ -integral ( $J_c$ ) which is less restrictive than the E399 requirement in many cases:

$$a, b, B \geq \frac{200 J_c}{\sigma_0} \quad (3)$$

This requirement derives from current research [6,7,8] examining the effects of constraint on fracture toughness. Experimental verification of Eq (3) would increase the applicability of measured fracture toughness values. For most metals, valid fracture toughness values can be obtained with smaller specimens. This paper re-examines the key data sets used to set the original 2.5 factor in the E399 requirement. By using  $J_c$ , rather than  $K_{Ic}$ , as the measure of fracture toughness, the widely varying ratio of Young's modulus to yield strength is reflected in the requirements. For high strength-low modulus metals (e.g. titanium) Eq (1) and (3) are nearly identical. However, for lower strength-high modulus metals (e.g. structural steels), Eq (3) more closely agrees with the 1.0 multiplier in Eq (1). The comparisons here demonstrate that Eq (3) maintains the strict requirement of the E399 expression for materials originally used to set the 2.5 factor while correctly relaxing the size requirement for other metals, most notably structural and pressure vessel ferritic steels.

### 3. THEORETICAL BACKGROUND

Much recent work [6,8,9,10] in fracture mechanics focuses on quantifying the kinematic constraint against plastic flow at the crack tip to predict the effects of finite component size on fracture toughness. Two approaches of particular interest are the DA micromechanics constraint model, and the  $J$ - $Q$  theory to describe crack tip fields as developed by O'Dowd and Shih [8,9]. These approaches determine the level of loading, relative to specimen size, when global plasticity impinges on the small scale yielding (SSY) crack tip fields. Once global plasticity affects the near tip fields, the unique coupling between  $J$ ,  $K_I$  and the near tip fields is lost and specimen size (and geometry) influences the measured fracture toughness. The size requirements given in Eq (3) were first proposed by DA and, as will be shown here, are corroborated by the  $J$ - $Q$  methodology.

#### 3.1 Dodds-Anderson Micromechanics Model

DA quantify the geometric effects on fracture toughness by coupling the global failure parameter ( $J_c$ ) with a micromechanics based failure model. The model is designed for ferritic materials in the ductile to brittle transition region thereby limiting the fracture mechanism to transgranular cleavage. For this failure mechanism, several micromechanical models have been recently proposed [11, 12, 13]. These

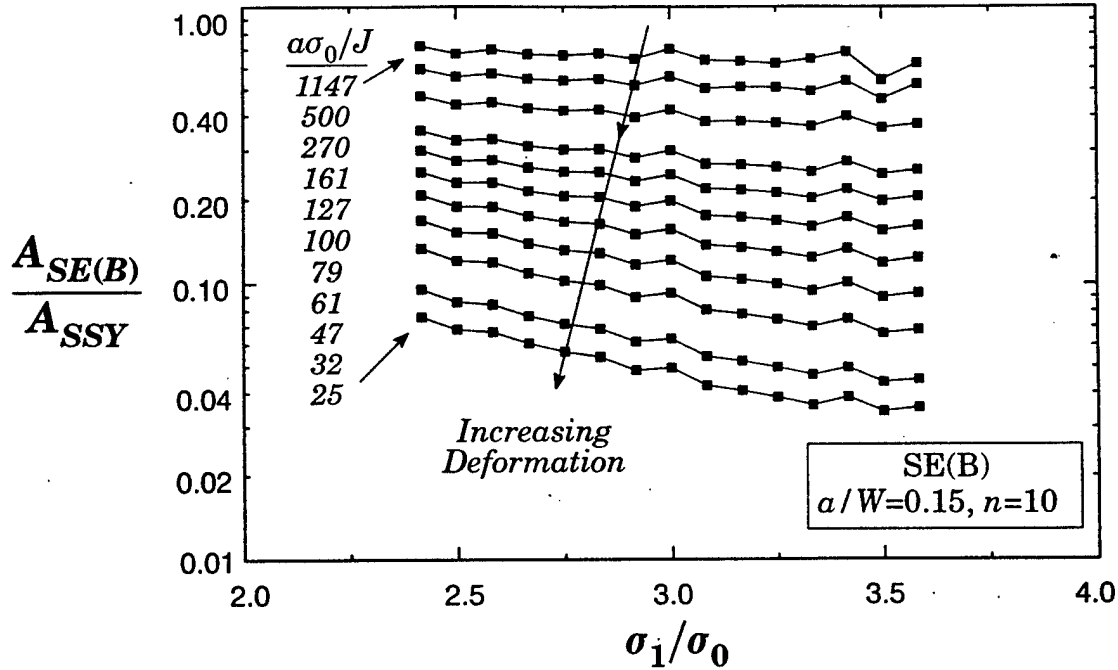


FIG. 1—Areas within principal stress contours for an  $a/W = 0.15$ ,  $n=10$  SE(B). Values are normalized by area within contour for SSY at same  $J$ -value.

models assume a favorably oriented particle (e.g. carbide or inclusion) initiates cleavage fracture. Failure of this particle creates a microcrack which triggers global fracture through a local Griffith instability. The sampling effects for a favorably oriented particle to create the initial microcrack suggests that the highly stressed volume of material ahead of the crack plays a dominant role. These features lead to adoption of the volume of material ahead of the crack over which the normalized principal stress ( $\sigma_1/\sigma_0$ ) exceeds a critical value as the local failure parameter. In plane-strain, the volume is simply the area ( $A$ ) within a principal stress contour  $\times$  the thickness ( $B$ ). Dimensional analysis [5] demonstrates that

$$A(\sigma_1/\sigma_0) \propto \frac{J^2}{\sigma_0^2} \quad (4)$$

DA use nonlinear finite element analyses of plane strain models to calculate areas within principal stress contours ahead of a crack tip. The analyses reveal that as deformation applied to a single edge notch bend (SE(B)) specimen increases, the area within a stress contour ahead of the crack tip increases but at a lesser rate (due to constraint loss) than the small-scale yielding (SSY) limit (Fig. 1). As is apparent from the nearly horizontal lines in Figure 1, the level of deviation from SSY is essentially independent of the critical principal stress contour until large amounts of deformation. These analyses define deformation levels beyond which specimen dimensions influence the relationship between applied- $J$  and area within a principal stress contour which drives the cleavage fracture (i.e. the measured  $J_c$  values become a function of specimen geometry). The area ratio is recast in terms of  $J$  as,

$$\frac{J_{SE(B)}}{J_{SSY}} = \sqrt{\frac{A_{SSY}}{A_{SE(B)}}} \quad (5)$$

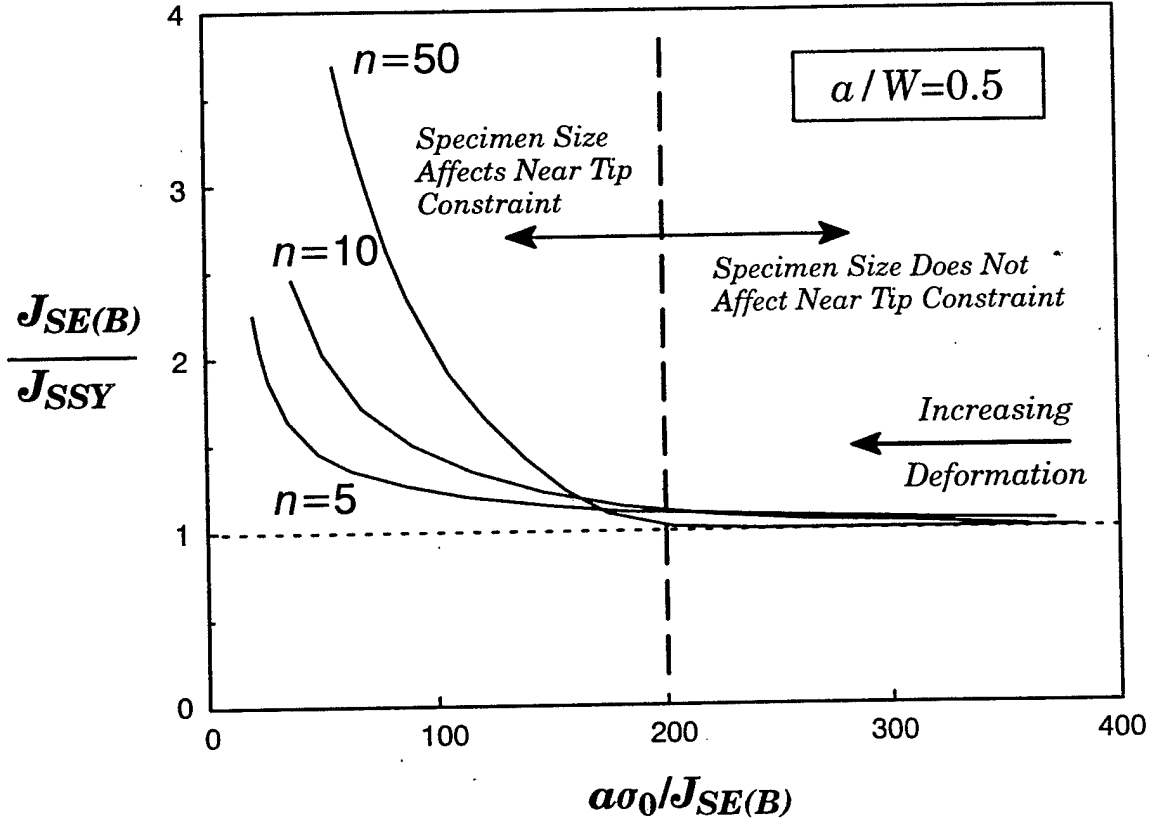


FIG. 2—Variation of finite body-to-SSY  $J$  with applied load for various strain hardening exponents in an  $a/W = 0.5$  SE(B) specimen.

DA calculate the ratio of  $J$  in the finite size specimen ( $J_{SE(B)}$ ) to the  $J$  under small-scale yielding conditions ( $J_{SSY}$ ) which generates equivalent stressed areas in the SE(B) ( $A_{SE(B)}$ ) and SSY ( $A_{SSY}$ ) conditions. The ratio  $J_{SE(B)}/J_{SSY}$  quantifies the deviation from SSY conditions. Figure 2 shows the variation of this ratio with applied load and strain hardening exponent and illustrates the basis for the size requirement on in-plane dimensions ( $a$  and  $b$ ) expressed by Eq (3). At low deformation levels, plasticity in the SE(B) specimen is well contained (i.e. small scale yielding); increases of  $J_{SE(B)}$  generate the same stressed volume of material as in SSY. As deformation increases, global plasticity affects the near tip stresses, and  $A_{SE(B)}$  increases at a substantially slower rate than  $A_{SSY}$ . As is apparent from Figure 2, the ratio  $J_{SE(B)}/J_{SSY}$  begins to increase rapidly above unity at a non-dimensional deformation of 200. The crack length provides a meaningful length to scale the level of plastic deformation relative to the in-plane size of the specimen. 3D finite element analyses of SE(B) specimens by Narasimhan and Rosakas [14], and Faleskog [15], indicate that thicknesses,  $B$ , satisfying Eq (3) also maintain SSY conditions.

### 3.2 $J$ - $Q$ Theory

The  $J$ - $Q$  description of crack tip fields derives from consideration of the Modified Boundary Layer (MBL) solution [16] which expresses near tip stresses for linear elastic plane strain conditions in the form,

$$\sigma_{ij} = \frac{K_I}{\sqrt{2\pi r}} \tilde{f}_{ij}(\theta) + T\delta_{1i}\delta_{1j} \quad (6)$$

where  $T$  is the non-singular stress parallel to the crack plane. The  $T$ -stress term does not affect  $K_I$  or  $J$ ; however, Larsson and Carlsson [17] demonstrate the second term significantly affects the plastic zone shape and size under SSY conditions. In finite-sized specimens the elastic  $T$ -stress, which varies proportionally with  $K_I$ , becomes ambiguous under conditions of large scale yielding as  $K_I$  saturates to a constant value at limit load.

O'Dowd and Shih [8,9] use asymptotic and finite element analyses to develop an approximate two-parameter description of the crack tip fields without the limitations of the  $T$ -stress,

$$\sigma_{ij} = \sigma_0 f_{ij}\left(\frac{r}{J/\sigma_0}, \theta; Q\right); \quad (7)$$

$$\epsilon_{ij} = \epsilon_0 g_{ij}\left(\frac{r}{J/\sigma_0}, \theta; Q\right). \quad (8)$$

The second term,  $Q$ , in Eqs (7,8) is the mechanism by which  $\sigma_{ij}$  and  $\epsilon_{ij}$  of an SE(B) differ from the SSY solution at the same applied- $J$ . O'Dowd and Shih [8,9] determined that, to a good approximation,  $Q$  represents a uniform hydrostatic stress in the forward sector ahead of the crack tip,  $|\theta| < \pi/2$  and  $J/\sigma_0 < r < 5J/\sigma_0$ . Operationally,  $Q$  is defined as

$$Q \equiv \frac{(\sigma_{\theta\theta})_{SE(B)} - (\sigma_{\theta\theta})_{SSY}}{\sigma_0}, \quad \text{at } \theta = 0, r = 2J/\sigma_0 \quad (9)$$

where stresses in Eq (9) are evaluated from plane strain finite element analyses containing sufficient mesh refinement to resolve the fields within the process zone for ductile and brittle fracture. At low deformation levels, the finite body is under SSY conditions and  $Q$  remains very nearly zero; however, under large-scale yielding conditions stresses at the crack tip are substantially less than those in SSY at the same  $J$ -values. This difference leads to negative  $Q$  values once the SE(B) specimen deviates from SSY conditions (Fig. 3). For deep notch bend specimens  $Q$  remains slightly positive at deformation corresponding to  $a\sigma_0/J_c > 200$ .

The  $J$ - $Q$  description of crack-tip stress and strain fields expressed in Eqs (7,8) provides the needed justification to apply the requirements of Eq (3) to materials that do not necessarily fracture by the purely stressed controlled, transgranular cleavage mechanism of the DA model. Satisfaction of the size/deformation requirements in Eq (3) insures that both the stress and strain fields at fracture correspond to SSY and are unaffected by the global response of the specimen. Consequently, the specific details of the fracture micromechanism (stress vs. strain controlled) become unimportant since  $J$  (or  $K_I$ ) uniquely defines both fields.

### 3.3 Statistical Thickness Effects

Previous experimental and theoretical work [20,21] on cleavage fracture in ferritic steels demonstrates an absolute thickness effect on fracture toughness not related to constraint. Metallurgical variations in the material along the crack front require a statistical treatment of thickness in experimental fracture toughness data. Wallin

[21] employs weakest link statistics to obtain the following statistical correction for fracture toughness data for specimens of different thickness ( $B$  and  $B_0$ ) which fail by cleavage without previous ductile tearing,

$$K_{\text{corr}} = K_{\text{min}} + (K_q - K_{\text{min}}) \left( \frac{B}{B_0} \right)^{1/4} \quad (10)$$

Recasting Eq (10) in terms of  $J$  yields,

$$J_{\text{corr}} \approx J_c \left( \frac{B}{B_0} \right)^{1/2} \quad (11)$$

The corrections given in Eqs (10,11) arise solely from the increased volume of material sampled along the crack front due to increased thickness. Each point along the crack front is *assumed* to be stressed at the same level. As the sampled volume increases, the probability of finding a metallurgical weak link increases. Because the failure of a weak metallurgical defect controls cleavage fracture, fracture toughness decreases with increasing probability of finding a defect.

The statistical assumptions employed to obtain Eqs (10,11) preclude application to materials which do not fracture by weakest link mechanisms. Consequently, the remainder of this presentation addresses only the deterministic effects of specimen size (i.e. constraint) on measured values of fracture toughness. Statistical treatment of fracture data, for example the thickness effect of sampled volume, should be ap-

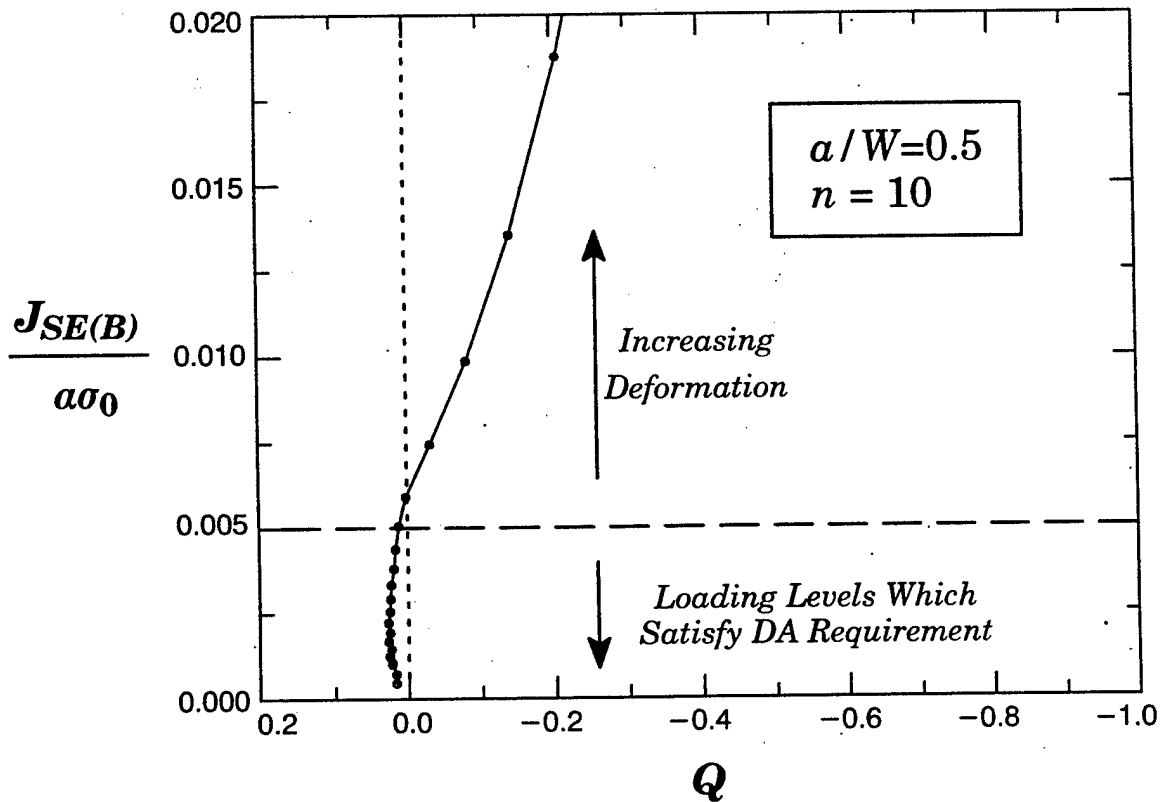


FIG 3.—Variation of  $Q$  with applied load for an  $a/W=0.5$  SE(B).

plied only to data that first meet the deterministic requirements for specimen size that maintain constraint.

**Table 1—References for Experimental Data**

Material	Reference
4340 Steel (399°C Temper)	Jones and Brown, <i>ASTM STP 463</i> , 1970, pp 63–101
Ti 6Al–6V–2Sn	Jones and Brown, <i>ASTM STP 463</i> , 1970, pp 63–101
18Ni Maraging Steel	Rolfe and Novack, <i>ASTM STP 463</i> , 1970, pp 94
A36 Steel	Sorem, <i>et. al</i> , <i>International Journal of Fracture</i> , Vol. 47, pp. 105–126, 1991.
A533B Class 1 Steel	McCabe, <i>ASTM STP 1189</i> , 1991, pp. 80–94

## 4. EVALUATION OF SIZE REQUIREMENTS

### 4.1 Materials and basis of comparison

Five experimental data sets spanning a variety of metals are considered in the comparison. Table 1 lists the materials along with the original references for the data. To compare the current E–399 and proposed size requirements for these metals, it is necessary to express them using the same fracture toughness parameter. Equation (3) is converted into terms of  $K$  using the SSY conversion for plane strain conditions,

$$J = \frac{K^2}{E/(1 - \nu^2)} \quad (12)$$

After converting Eq (3) to  $K$  and expressing  $\sigma_0$  in terms of  $\sigma_{ys}$  and  $\sigma_{uts}$ , the DA size requirement is expressed as

$$L_{200} \geq \frac{400 K_q^2 (1 - \nu^2)}{E(\sigma_{ys} + \sigma_{uts})} \quad (13)$$

$L_{200}$  refers to the minimum specimen size (i.e.  $a, b, B$ ). With both size requirements expressed using the same fracture toughness parameter, their ratio becomes a function of material properties,

$$\frac{L_{200}}{L_{E399}} = \frac{160 (1 - \nu^2) \sigma_{ys}^2}{E (\sigma_{ys} + \sigma_{uts})} \quad (14)$$

This ratio quantifies the change in minimum specimen size afforded by the proposed size requirement for a specific material. A value of  $L_{200} / L_{E399}$  less than unity indicates that the proposed size requirement is less restrictive than the current E399 requirement. Table 2 lists, in ascending order, this size ratio for the five metals. The decrease in specimen size requirement ranges from a factor of 16 for A36 steel to 1.4 for Ti 6Al–6V–2Sn. The proposed size requirement is less restrictive than the E399 for all metals considered in Table 1, but only slightly so for the titanium alloy.



**Table 2—Material properties and size ratios for experimental data**

Material	Yield [MPa]	Ultimate [MPa]	Modulus [GPa]	Poisson's ratio	$L_{200}/$ $L_{E399}$
A36 Steel	248	460	207	0.3	0.06
A533B Class 1 Steel	407	559	207	0.3	0.12
18Ni Maraging Steel	1323	1379	207	0.3	0.46
4340 Steel (399°C Temper)	1468	1538	207	0.3	0.49
Ti 6Al-6V-2Sn	1200	1269	117	0.32	0.71

## 4.2 Experimental data

The five experimental data sets are examined in the order given in Table 2. Fracture toughness is plotted against the relevant specimen dimension. Two lines designated  $L_{200}$  and  $L_{E399}$  appear on each plot and represent the size requirements (deformation limits) for E399 (solid line) and DA (dashed line). Fracture toughness values below (and to the right of) each line satisfy the corresponding size/deformation limit. Single and double arrows appear on the  $L_{200}$  line in each plot for emphasis. Data points on the single arrow side of the  $L_{200}$  line require a constraint correction as proposed by DA [22]; data points on the double arrow side satisfy the  $L_{200}$  size/deformation limit but may require a statistical thickness correction. Double arrows appear on the  $L_{E399}$  line to emphasize the region over which data satisfies the E399 criterion.

The A36 data set [23] consists of SE(B) specimens with a variety of crack depth, thickness, and width-to-thickness ( $W/B$ ) ratios tested at  $-76^{\circ}\text{C}$ . The  $J$  at cleavage,  $J_c$ , is given for two thickness ( $B = 12.7$  and  $31.75$  mm). Figure 4 provides this data. Both thicknesses contain specimens with three different  $W/B$  ratios as indicated by the different symbols. This material has the largest difference between  $L_{E399}$  and  $L_{200}$ ; application of the E399 size requirement indicates the entire data set is specimen size dependent. All of the  $B = 31.75$  mm data and several of the data points with  $B = 12.7$  mm meet the proposed size requirement of DA. The total data set shows a significant increase in toughness with decreasing thickness; however, the  $L_{200}$  criterion successfully separates data points which show an increase in fracture toughness due to large scale yielding effects from specimen size insensitive data. Figure 5 shows the variation of fracture toughness with crack depth for the same data set. The  $L_{200}$  criterion successfully indicates  $J_c$  values dependent on crack depth; the E399 criterion indicates that all data values are size/deformation dependent (which does not appear to be correct for this data set).

Figure 6 shows fracture toughness values for an A533B Class 1 steel. The data includes 1/2T, 1T, 2T and 4T C(T) specimens tested at  $-75^{\circ}\text{C}$ . For this data set, the fracture toughness is plotted using  $K_{Jc}$  values obtained by converting measured  $J_c$  values using Eq (12). The proposed size requirement again indicates data points which cause the data set to show an increase in fracture toughness with decreasing thickness.

Deep notch SE(B) specimens of two thicknesses ( $W = 102$  and  $152$  mm) provide fracture toughness data for 18 Ni maraging steel (Fig. 7). Rolfe and Novak use this data to argue for a reduction of the multiplier in E399 from 2.5 to 1.0. Fracture toughness values are clearly specimen size independent for thickness greater than

approximately  $B = 10$  mm. The thickness requirement given by the  $L_{200}$  curve agrees with the recommendations of Rolfe and Novak.

Fracture toughness values for a 4340 steel shown in Figures 8, 9 and 10 were obtained from a series of tests conducted on specimens removed from a 25.4 mm thick, hot-rolled and annealed plate. The specimen blanks were heat treated in a neutral salt bath at 843°C for 1/2 hour, oil quenched, and tempered at 399°C for one hour. The SE(B) specimens comprised three different widths ( $W = 56, 25.4,$  and 14 mm) each having initial  $a/W = 0.5$ . Only the  $W = 14$  mm data set reveals significant variations in  $K_Q$  with thickness (Fig. 10). The rapid decrease in toughness with decreasing thickness which is observed in this data set may be due to the very thin specimens (e.g.  $B = 3.8$  mm). Once the specimen thickness decreases beyond a critical point, fracture toughness decreases due to the reduction of material available for plastic energy dissipation. The DA size requirement indicates all data points showing specimen size dependency.

The high yield strength coupled with the low value of Young's modulus for Ti 6Al-6V-2Sn causes the  $L_{200}/L_{E399}$  ratio to be significantly nearer to unity for this material than for the other four materials listed in Table 1. The titanium data (Fig. 11) shows a rapid increase in fracture toughness with decreasing thickness; this rapid upswing in toughness caused Jones and Brown [4] to argue (successfully) for the

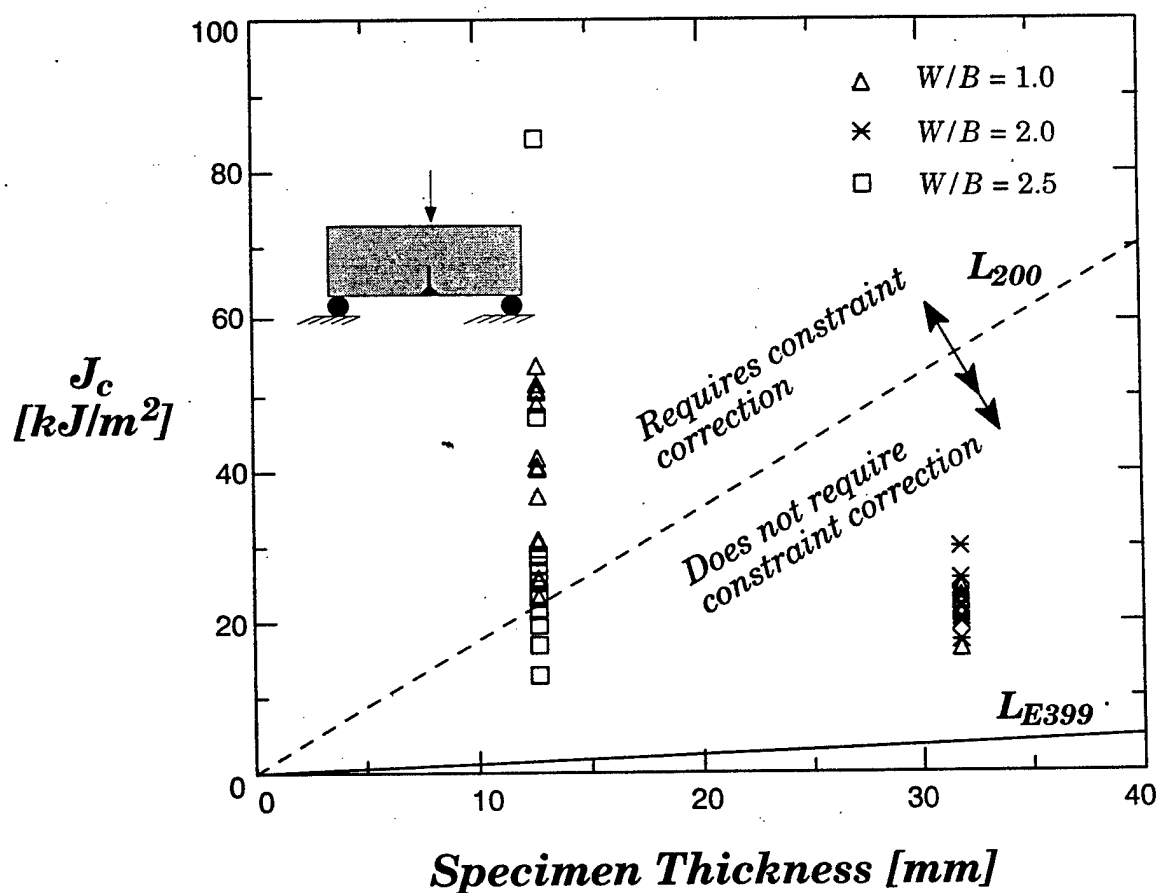


FIG. 4—Variation of fracture toughness with specimen thickness for A36 steel at  $-76^{\circ}\text{C}$ .

more restrictive 2.5 multiplier in the E399 size requirement. The proposed size limit designates as size insensitive an additional data point beyond the E399 limit.

## 5. SUMMARY AND DISCUSSION

This paper offers experimental verification of the DA size requirements for brittle fracture given in Eq (3). DA originally proposed these requirements for materials that fracture by transgranular cleavage. Subsequent development of the  $J$ - $Q$  methodology generalizes the work of DA by removing the restriction of a stress-controlled, cleavage mechanism. The proposed size requirements are shown, using finite element analyses, to quantify the deformation limits under which conditions of small-scale yielding ( $T = 0$ ) exist at the crack tip with both stress and strain fields uniquely characterized by  $J$ .

The proposed size requirements are examined for five existing data sets of fracture toughness which span properties between low strength-high modulus (A36) and high strength-low modulus (titanium). The proposed requirements successfully indicate toughness values in each data set which exhibit size dependency due to a loss of kinematic constraint against plastic deformation. The new size requirement is much less restrictive than the current E399 size requirement for materials with a low strength and high modulus, e.g., common structural and pressure vessel steels. For materials with a higher strength but lower modulus, e.g., the titanium alloy, the new requirement is just marginally less restrictive (the titanium alloy examined here played a key role is setting the E399 factor of 2.5). By expressing the fracture

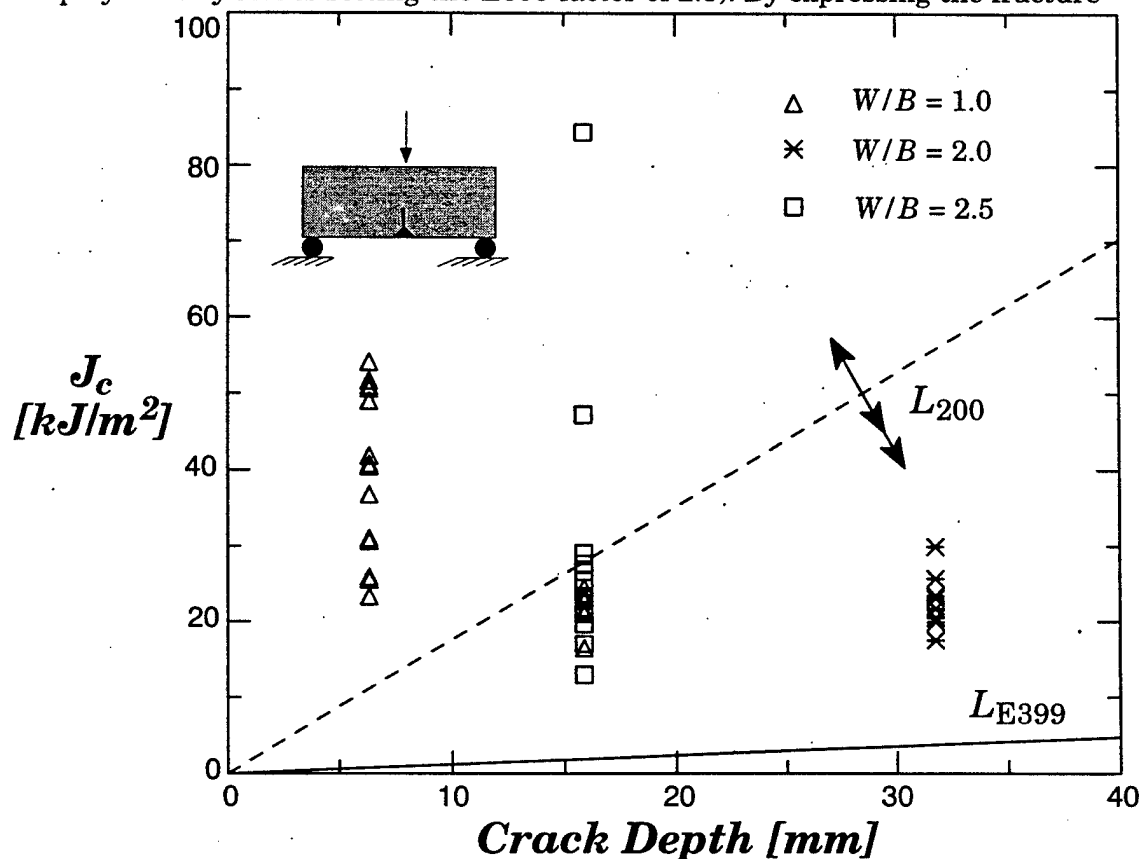


FIG. 5—Variation of fracture toughness with crack depth for A36 steel at  $-76^\circ\text{C}$ .

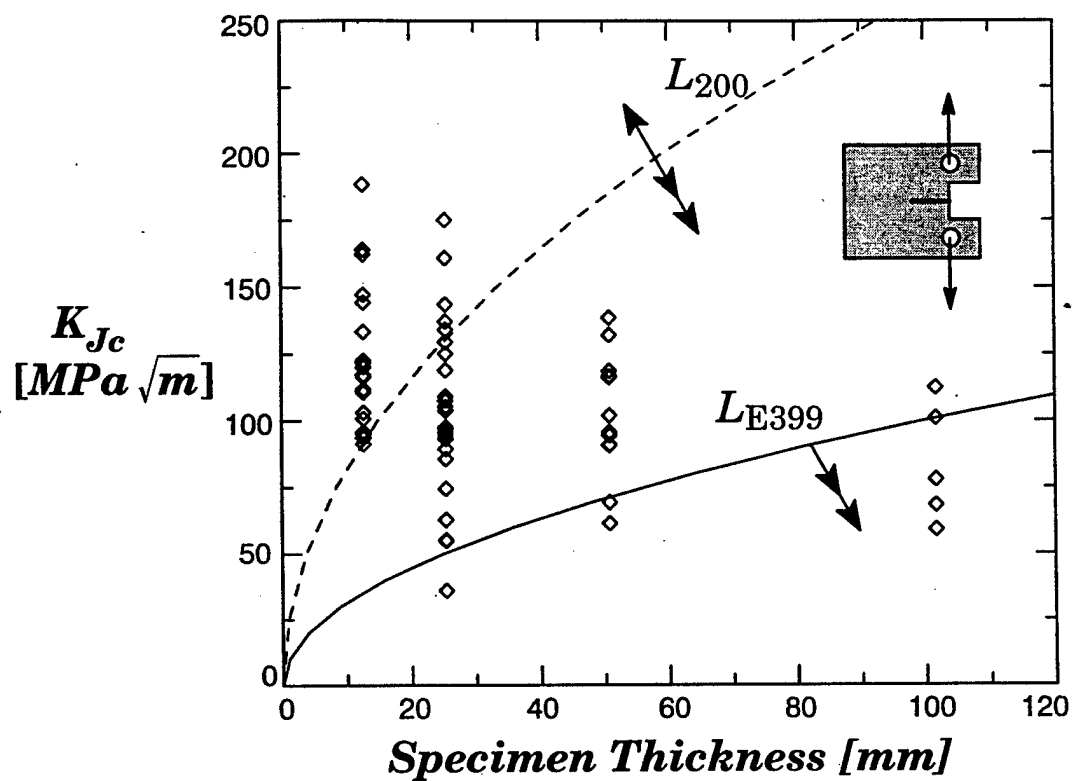


FIG. 6—Variation of fracture toughness with specimen thickness for A533-B at -75°C.

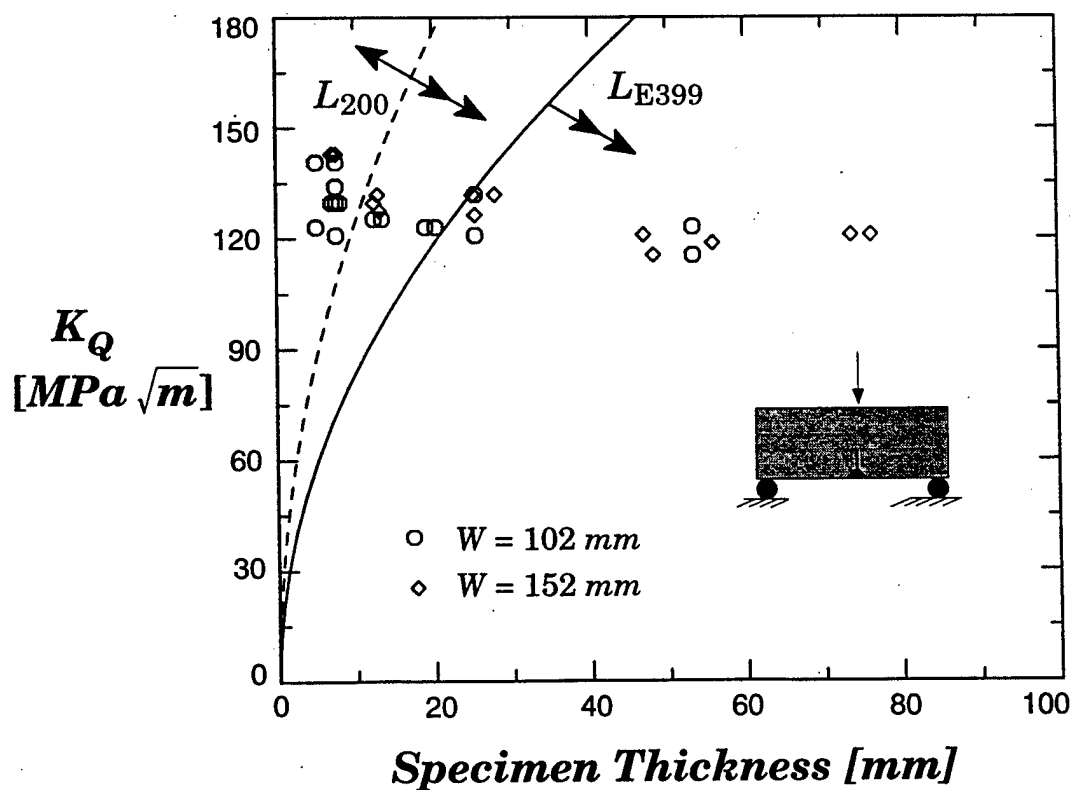


FIG. 7—Variation of fracture toughness with thickness for 18 Ni maraging steel.

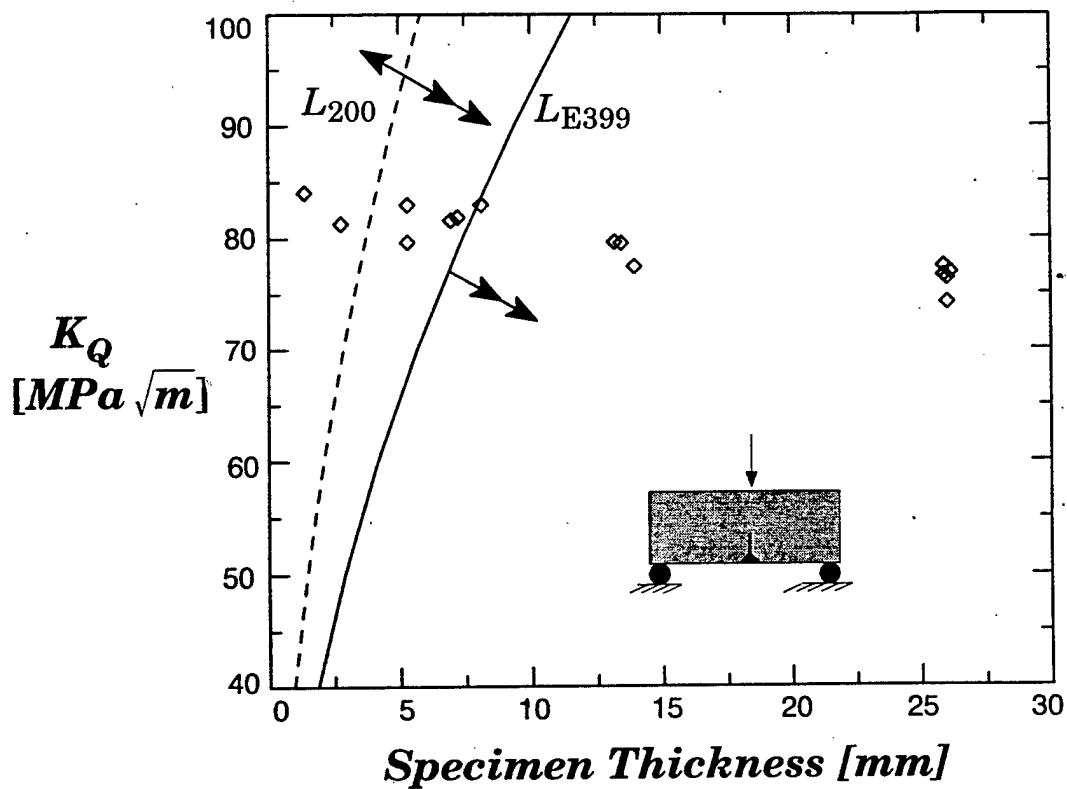


FIG. 8—Variation of fracture toughness with specimen thickness for 4340 steel  $a_0 = 28$  mm,  $W = 56$  mm.

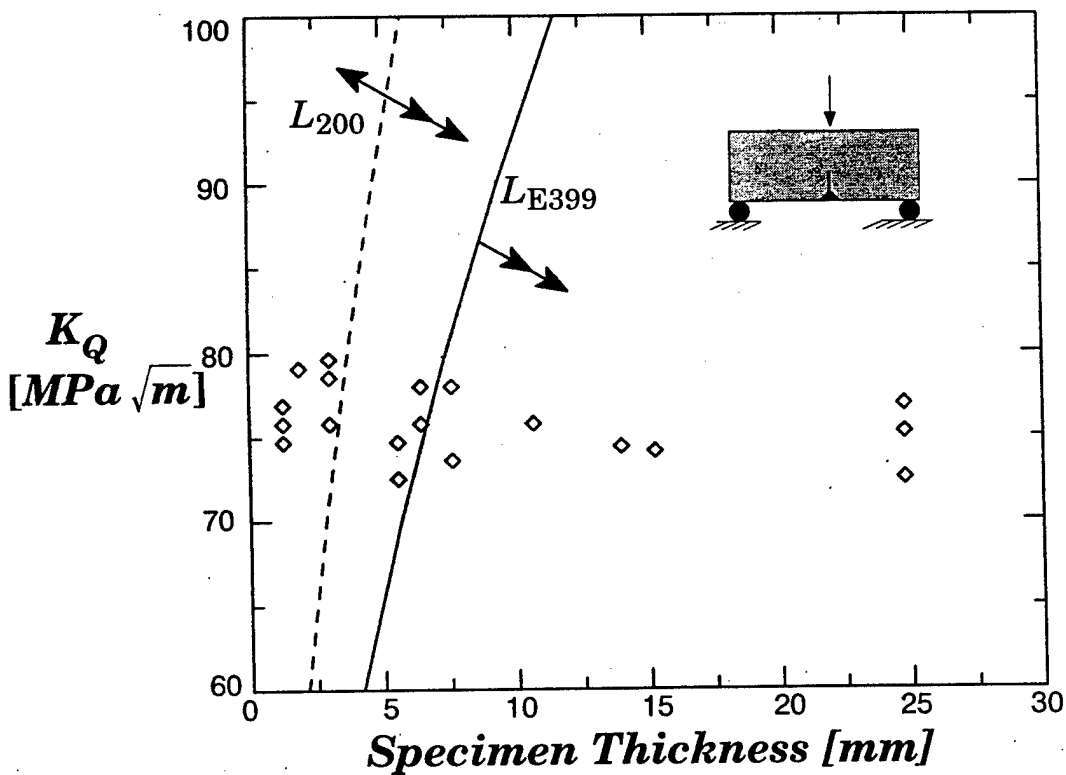


FIG. 9—Variation of fracture toughness with specimen thickness for 4340 steel  $a_0 = 12.7$  mm,  $W = 25.4$  mm.

toughness in terms of  $J$ , the strong influence of Young's modulus relative to strength is correctly reflected in the proposed size requirements.

Recent work by Faleskog [15], and work-in-progress by the authors suggests that the size requirements might be reduced to

$$a, b, B \geq \frac{100 J_c}{\sigma_0} \quad (15)$$

for deeply cracked SE(B) specimens of materials having a low yield strength and high Young's modulus which includes most structural and pressure vessel steels. A similar reduction in size requirements for alloys possessing high yield strength to Young's modulus ratios, such as Titanium 6Al-6V-2Sn, may not be possible. Three-dimensional finite element analyses reveal that the centerplane in SE(B) specimens (with  $B=W$ ;  $B=W/2$ ) and standard C(T) specimens maintains small-scale yielding conditions at deformation levels greater than the plane-strain limit of Eq (3). Away from the centerplane, crack-tip conditions become less constrained which introduces the complexity of defining an "equivalent" thickness to quantify constraint levels. Additional experimental data from Wallin [21] on pressure vessel steels also supports size requirements suggested by Eq (15). Nevertheless, it is clear that the proposed size requirements in Eq (3) are conservative for these materials and specimen geometries and that on-going work may provide sufficient justification to adopt Eq (15) for ferritic materials.

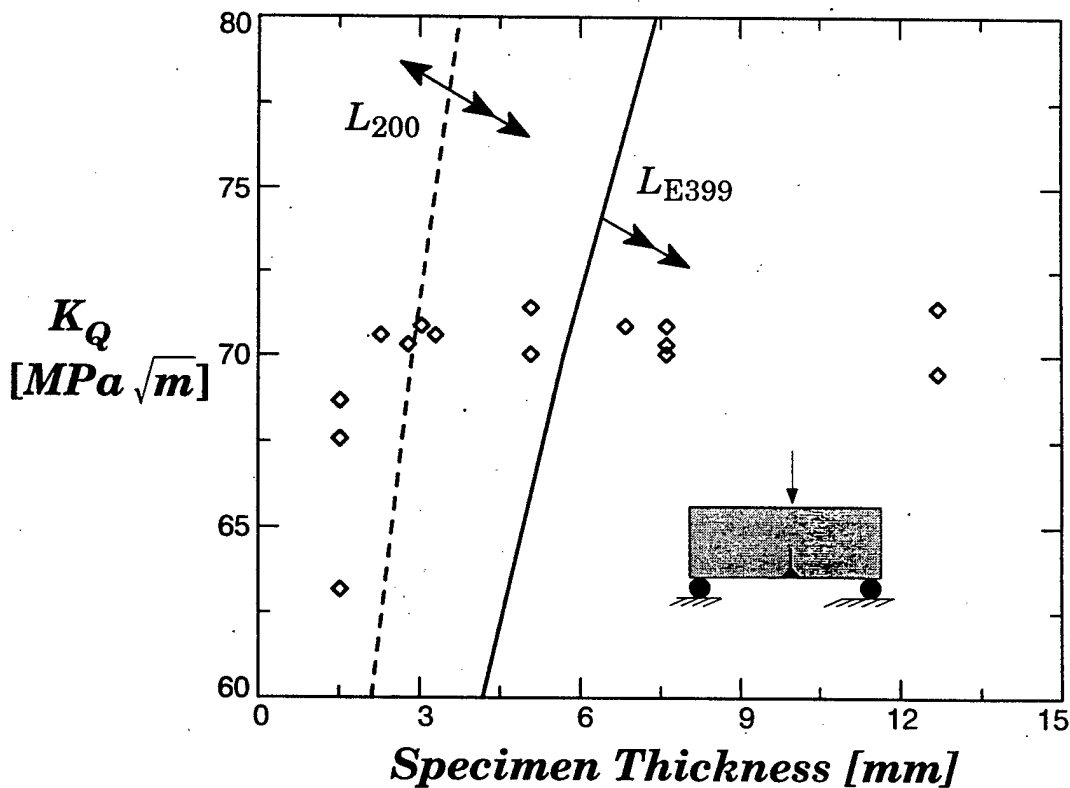


FIG. 10—Variation of fracture toughness with specimen thickness for 4340 steel,  $a_0 = 6.9$  mm,  $W = 14$  mm.

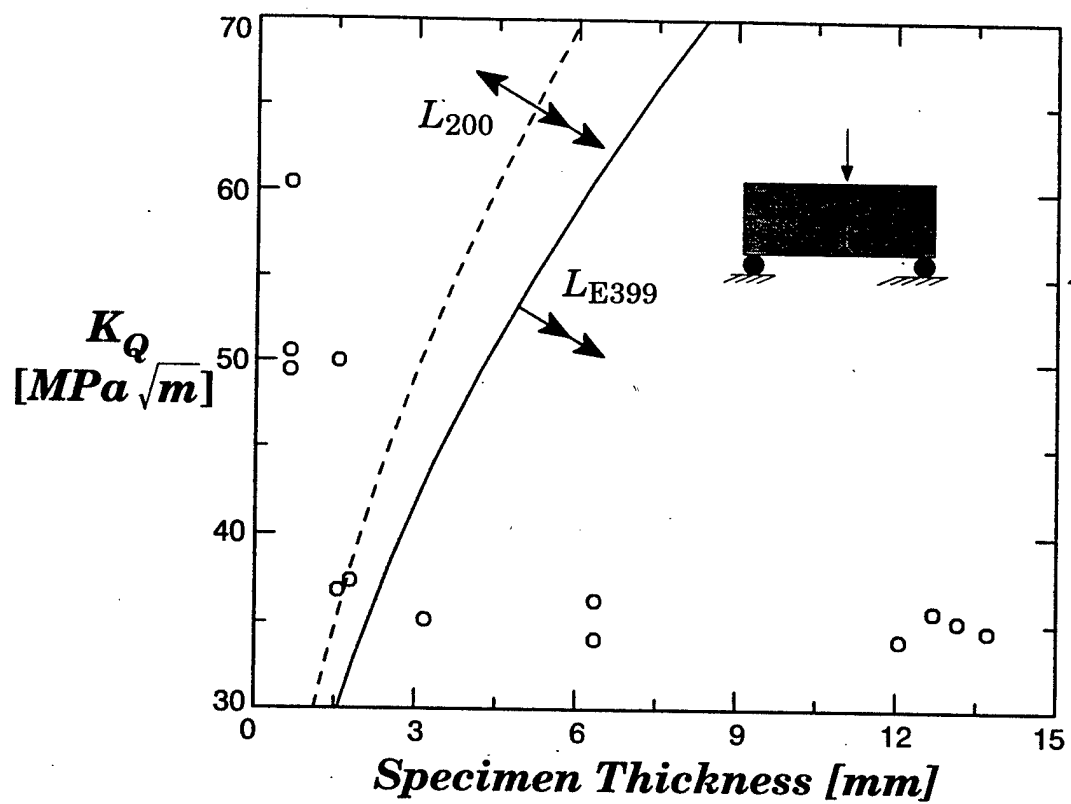


FIG. 11—Variation of fracture toughness with thickness for Ti 6Al-6V-2Sn.

## 6. REFERENCES

- [1] ASTM E399: "Standard Test Method for Plane-Strain Fracture Toughness of Metallic Materials," American Society of Testing and Materials, Philadelphia, 1990.
- [2] Rolfe, S. T. and Novak, S. R., "Slow-Bend  $K_{Ic}$  Testing of Medium-Strength High-Toughness Steels," *Review of Developments in Plane Strain Fracture Toughness Testing*, ASTM STP 463 American Society for Testing and Materials, Philadelphia, 1970, pp. 124-159.
- [3] Facuher, B. and Tyson, W. R. "A Study of Variability, Size, and Temperature Effects on the Fracture Toughness of an Arctic-Grade Steel Plate," *Fracture Mechanics: Eighteenth Symposium*, ASTM STP 945, D. T. Read and R. P. Reed, Eds., American Society for Testing and Materials, Philadelphia, 1988, pp. 164-178.
- [4] Jones, M. H. and Brown, W. F., Jr., "The Influence of Crack Length and Thickness in Plane Strain Fracture Toughness Tests," *Review of Developments in Plane Strain Fracture Toughness Testing*, ASTM STP 463 American Society for Testing and Materials, Philadelphia, 1970, pp. 63-101.
- [5] Anderson, T. L. and Dodds, R. H., Jr., "Specimen Size Requirements for Fracture Toughness Testing in the Transition Region," *Journal of Testing and Evaluation*, JTEVA, Vol. 19, No. 2, March 1991, pp. 123-134.
- [6] Dodds, R. H., Anderson, T. L., and Kirk, M. T., "A Framework to Correlate  $a/W$  Ratio Effects on Elastic-Plastic Fracture Toughness ( $J_c$ )," *International Journal of Fracture*, Vol. 48, pp. 1-22, 1991.
- [7] Hancock, J. W., Reuter, W. G., and Parks, D. M., "Constraint and Toughness Parameterized by  $T$ ," *Constraint Effects in Fracture*, ASTM STP 1171, E. M. Hackett, K.-H. Schwalbe, and R. H. Dodds, Eds., American Society for Testing and Materials, Philadelphia, Pennsylvania, pp. 21-40, 1993.
- [8] O'Dowd, N.P., and Shih, C.F., "Family of Crack-Tip Fields Characterized by a Triaxiality Parameter: Part I - Structure of Fields," *Journal of the Mechanics and Physics of Solids*, Vol. 39, No. 8, pp. 989-1015, 1991.
- [9] O'Dowd, N.P., and Shih, C.F., "Family of Crack-Tip Fields Characterized by a Triaxiality Parameter: Part II - Fracture Applications," *Journal of the Mechanics and Physics of Solids*, Vol. 40, pp. 939-963, 1992.
- [10] Sumpter, J. D. G., and Forbes, A. T., "Constraint Based Analysis of Shallow Cracks in Mild Steel," *Proceedings of the International Conference on Shallow Crack Fracture Mechanics Tests and Applications*, TWI, Cambridge, England, September 1992.
- [11] Anderson, T. L. and Stienstra, D., "A Model to Predict the Sources and Magnitude of Scatter in Toughness Data in the Transition Region," *Journal of Testing and Evaluation*, JTEVA, Vol. 17, 1989, pp. 46-53.
- [12] Lin, T., Evans, A. G., and Ritchie, R. O., "Statistical Model for Carbide Induced Brittle Fracture in Steel," *Journal of the Mechanics and Physics of Solids*, Vol. 34, 1986, pp. 477-496.
- [13] Beremin, F. M., "A Local Criterion for Cleavage Fracture of a Nuclear Pressure Vessel Steel," *Metallurgical Transactions A*, Vol. 14A, 1983, pp. 2277-2287.
- [14] Narasimhan, R. and Rosakis, A. J., "Three Dimensional Effects Near a Crack Tip in a Ductile Three Point Bend Specimen - Part I: A Numerical Investigation," Report SM 88-6, California Institute of Technology, Division of Engineering and Applied Sciences, Pasadena, Calif., Jan. 1988
- [15] Faleskog, J., "Effects of Local Constraint Along Three Dimensional Crack Fronts - A Numerical and Experimental Investigation," Report 163, TRITA-HFL-0163 ISSN 0281-1502, Department of Solid Mechanics, Royal Institute of Technology, S-100 44, Stockholm, Sweden.
- [16] Williams, M. L., *Journal of Applied Mechanics*, Vol. 24, pp. 109-114, 1957.
- [17] Larsson, S. G., and Carlsson, A. J., "Influence of Non-Singular Stress Terms and Specimen Geometry on Small-Scale Yielding at Crack Tips in Elastic-Plastic Materials," *Journal of Mechanics and Physics of Solids*, Vol. 21, 1973, pp. 263-278.



- [18] McCabe, D. E. "A Comparison of Weibull and  $\beta_{Ic}$  in Transition Range Data," *Fracture Mechanics: Twenty-Third National Symposium, ASTM STP 1189*, American Society of Testing and Materials, Philadelphia, 1993, pp. 80-94.
- [19] Ritchie, R. O., and Thompson, A. W., *Metallurgical Transactions A*, Vol. 16A, pp. 233-248, 1985.
- [20] Wallin, K., "The Effect of Ligament Size on Cleavage Fracture Toughness," *Engineering Fracture Mechanics*, Vol. 32, 1989, pp. 449-457.
- [21] Wallin, K., "Statistical Aspects of Constraint with Emphasis on Testing and Analysis of Laboratory Specimens in the Transition Region," *Constraint Effects in Fracture, ASTM STP 1171*, E. M. Hackett, K. H. Schwalbe, and R. H. Dodds, Eds., American Society of Testing and Materials, 1993, pp. 264-288.
- [22] Dodds, R. H., Anderson, T. L., and Kirk, "A Framework to Correlate  $a/W$  Ratio Effects on Elastic-Plastic Fracture Toughness ( $J_c$ )," *International Journal of Fracture*, Vol. 48, 1991, pp. 1-22.
- [23] Sorensen, W. A., Dodds, R. H., and Rolfe, S. T., "Effects of Crack Depth on Elastic Plastic Fracture Toughness," *International Journal of Fracture*, Vol. 47, pp. 105-126, 1991.

**BIBLIOGRAPHIC DATA SHEET**

(See instructions on the reverse)

1. REPORT NUMBER  
(Assigned by NRC, Add Vol., Supp., Rev.,  
and Addendum Numbers, if any.)

NUREG/CR-6191

2. TITLE AND SUBTITLE

SIZE AND DEFORMATION LIMITS TO MAINTAIN CONSTRAINT IN  
 $K_{Ic}$  AND  $J_c$  TESTING OF BEND SPECIMENS

3. DATE REPORT PUBLISHED

MONTH YEAR  
October 1995

4. FIN OR GRANT NUMBER

J6036

5. AUTHOR(S)

KYLE C. KOPPENHOEFER, UNIVERSITY OF ILLINOIS  
ROBERT H. DODDS, JR., UNIVERSITY OF ILLINOIS

6. TYPE OF REPORT

TECHNICAL

7. PERIOD COVERED (Inclusive Dates)

1/1/93 - 12/31/93

8. PERFORMING ORGANIZATION - NAME AND ADDRESS (If NRC, provide Division, Office or Region, U.S. Nuclear Regulatory Commission, and mailing address; if contractor, provide name and mailing address.)

UNIVERSITY OF ILLINOIS  
DEPARTMENT OF CIVIL ENGINEERING, MC-250  
205 NORTH MATHEWS AVENUE  
URBANA, IL 61801-2352

UNDER CONTRACT TO:  
NAVAL SURFACE WARFARE CENTER  
ANNAPOLIS DETACHMENT, CARDEROCK DIV.  
CODE 6140, ANNAPOLIS, MD 21402-5067

9. SPONSORING ORGANIZATION - NAME AND ADDRESS (If NRC, type "Same as above"; if contractor, provide NRC Division, Office or Region, U.S. Nuclear Regulatory Commission, and mailing address.)

DIVISION OF ENGINEERING TECHNOLOGY  
OFFICE OF NUCLEAR REGULATORY RESEARCH  
U.S. NUCLEAR REGULATORY COMMISSION  
WASHINGTON, DC 20555-0001

10. SUPPLEMENTARY NOTES

NRC PROJECT MANAGER: SHAH N.M. MALIK

11. ABSTRACT (200 words or less)

The ASTM Standard Test Method for *Plane-Strain Fracture Toughness of Metallic Materials* (E399-90) restricts test specimen dimensions to insure the measurement of highly constrained fracture toughness values ( $K_{Ic}$ ). These requirements insure small-scale yielding (SSY) conditions at fracture, and thereby the validity of linear elastic fracture mechanics.

Recently, Dodds and Anderson have proposed a less restrictive size requirement for cleavage fracture toughness measured in terms of the J-integral ( $J_c$ ), as given by  $a, b, B \geq 200 J_c / \sigma_o$ . The size requirement proposed by Dodds and Anderson increases the applicability of fracture toughness experiments by expanding the range of conditions over which fracture toughness data meeting SSY conditions can be reliably measured. This investigation compares the proposed size requirement with that of ASTM Standard Test Method E399 and, by comparison with published experimental data for various alloys, provides validation of the new requirements.

12. KEY WORDS/DESCRIPTORS (List words or phrases that will assist researchers in locating the report.)

fracture toughness, specimen size requirements, experimental validation, J-integral

13. AVAILABILITY STATEMENT

unlimited

14. SECURITY CLASSIFICATION

(This Page)

unclassified

(This Report)

unclassified

15. NUMBER OF PAGES

16. PRICE